

**DIFFRACTION EFFICIENCY ENHANCEMENT OF
GUIDED OPTICAL WAVES BY MAGNETOSTATIC
FORWARD VOLUME WAVES IN THE
YTTRIUM-IRON-GARNET WAVEGUIDE COATED
WITH PERFECT METAL LAYERS**

F. Wen and B.-J. Wu

Key Lab of Broadband Optical Fiber Transmission and
Communication Networks of the Ministry of Education
University of Electronic Science and Technology of China
Chengdu 610054, P. R. China

Abstract—The diffraction efficiency (DE) of guided optical waves (GOWs) and the magneto-optic (MO) -3 dB bandwidth are key parameters in MO Bragg cells. To improve the diffraction performance, the MO Stokes interaction between magnetostatic forward volume waves (MSFVWs) and GOWs are studied by use of the coupled-mode theory in metal clad yttrium-iron-garnet (YIG) waveguides. Our analysis shows that, by adjusting the spacing of the metal layer from the ferrite surface, (1) the DE can be further increased by 7.32 dB compared with that of the inclined magnetization, but the MO bandwidth will be dropped down to the low level in the optimizing waveguide configuration; (2) when the DE and the MO bandwidth should be considered synthetically, a DE improvement of 3.9 dB with a bandwidth about 560 MHz is achieved corresponding to the large gain-bandwidth product. Thus, the YIG waveguide coated with perfect metal layers can be used to improve the performance of MO Bragg cells.

1. INTRODUCTION

The propagation characteristics of magnetostatic waves (MSWs) can be controlled by the spacing of the metal layer from the YIG film, which leads to tunable delay lines with linear [1] or constant [2, 3] dispersion. In addition, the diffraction efficiency (DE) of the guided optical waves (GOWs) should also be increased because the MSW power is concentrated in the magneto-optic (MO) interaction region

by the appearance of metal layers. Our calculation indicates that, the GOW diffraction efficiency by magnetostatic forward volume waves (MSFVWs) is increased by the metal layer effects, especially in the case of the inclined bias magnetic field. At the same time, the MSFVW frequency resolution which is the key parameter in the MO spectrum analyzer is also improved to a certain extent by metal layer effects. Consequently, the performance of MO Bragg cells can be enhanced by a proper selection of the spacing between the YIG film and metal layers.

In the paper we focus on the MO Bragg interaction in obliquely magnetized yttrium-iron-garnet/gadolinium-gallium-garnet (YIG/GGG) waveguides coated with perfect metal layers. The dependences of the Bragg DE, the corresponding frequency and the -3 dB bandwidth on the spacing of metal layers from the ferrite surface are investigated. And the maximum DE improvement of 7.32 dB is obtained when the spacing is equal to the thickness of the YIG film and the inclination angle θ is 15.5° . However, the MO bandwidth is obviously dropped down when metal layers are close to the YIG film. To appraise the performance of a practical MO Bragg cell comprehensively, the gain-bandwidth product is applied to evaluate the metal effects on the Bragg DE and the MO bandwidth. A 3.9 dB improvement with a bandwidth about 560 MHz is achieved when the gain-bandwidth product is up to the maximum, which keeps 70% MO bandwidth of the case without metal layers.

2. THE MO COUPLED-MODE THEORY IN METAL CLAD YIG WAVEGUIDES

In the paper the metal/dielectric/yttrium-iron-garnet (YIG)/gadolinium-gallium-garnet(GGG)/metal (MDYGM) structure is considered. The dispersion relation and the dynamic magnetization of MSFVWs are derived by the method of surface magnetic permeability. And the MO coupled-mode equations of the inclined magnetization are solved when phase-matching conditions are satisfied, which can help to find the relation between the GOW power and the MSFVW dynamic magnetization.

2.1. The Characteristics of MSFVW Propagation in the MDYGM Structure

The MDYGM waveguide consists of a YIG film grown by liquid phase epitaxy (LPE) method on a GGG substrate and the microstrip line transducers lift off the YIG film with the thickness l_1 , which is

sandwiched between two perfect metal layers, as shown in Fig. 1. \vec{H}_i is the effective internal direct current (dc) magnetic field, designated by (H_i, θ, φ) .

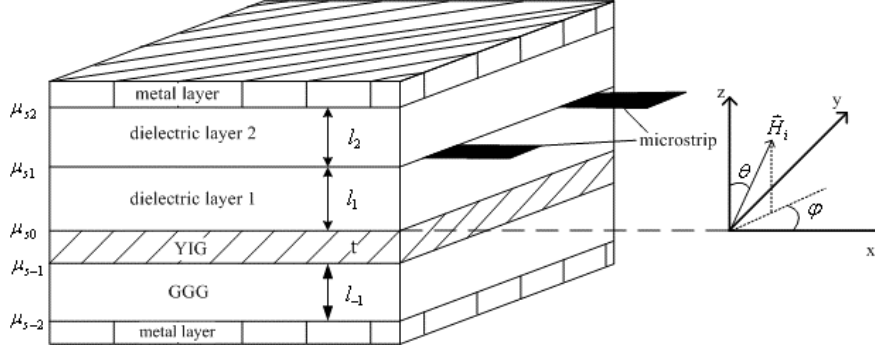


Figure 1. The configuration of the metal clad YIG waveguide.

Using the magnetostatic approximation [4] and the method of surface magnetic permeability defined by $\mu_s = -i \frac{b_z}{h_y}$ [5], the relations of surface magnetic permeabilities (see also Fig. 1) are derived as follows:

$$\mu_{s1} = -s\mu_0 \frac{-\mu_{s2} + s\mu_0 \tanh(sk_s l_2)}{s\mu_0 - \mu_{s2} \tanh(sk_s l_2)} \quad (1a)$$

$$\mu_{s0} = -s\mu_0 \frac{-\mu_{s1} + s\mu_0 \tanh(sk_s l_1)}{s\mu_0 - \mu_{s1} \tanh(sk_s l_1)} \quad (1b)$$

$$\mu_{s0} = \frac{upe^{\alpha_2 t} + vqe^{\beta_2 t}}{k_s(pe^{\alpha_2 t} + qe^{\beta_2 t})} \quad (1c)$$

$$\mu_{s-1} = s\mu_0 \frac{\mu_{s-2} + s\mu_0 \tanh(sk_s l_{-1})}{s\mu_0 + \mu_{s-2} \tanh(sk_s l_{-1})} \quad (1d)$$

where k_s is the MSW wavenumber, $s = k_s / |k_s|$, $\alpha_2 = ik_s \frac{(\mu_{23} + \mu_{32}) + s\sqrt{\Delta}}{2\mu_{33}}$, $\beta_2 = ik_s \frac{(\mu_{23} + \mu_{32}) - s\sqrt{\Delta}}{2\mu_{33}}$, $\Delta = (\mu_{23} + \mu_{32})^2 - 4\mu_{22}\mu_{33}$; $p = \mu_{s-1}k_s - v$, $q = u - \mu_{s-1}k_s$, $u = -i\mu_0\mu_{32}k_s + \mu_0\mu_{33}\alpha_2$, $v = -i\mu_0\mu_{32}k_s + \mu_0\mu_{33}\beta_2$; and the relative permeability components μ_{ij} ($i, j = 1, 2, 3$) are given in the Ref. [6].

The dispersion relation of MSFVWs can be obtained from the Equation (1c) : $|k_s| = \frac{\mu_{33}}{t\sqrt{\Delta}} [m\pi + 2 \tan^{-1}(\frac{a'}{b'})]$, ($m = 0, 1, 2 \dots$), where $a' = \frac{s\mu_0\sqrt{\Delta}}{2}(\mu_{s0} - \mu_{s-1})$, $b' = -\mu_0^2[\frac{|\Delta|}{4} + (\chi_a \cos \varphi \sin \theta)^2] - \mu_{s0}\mu_{s-1} - \mu_0\chi_a \cos \varphi \sin \theta(\mu_{s0} + \mu_{s-1})$, $\mu_{s0} = -s\mu_0 \tanh[sk_s(l_1 + l_2)]$, $\mu_{s-1} = s\mu_0 \tanh(sk_s l_{-1})$.

According to $\vec{m} = \vec{\chi} \cdot \vec{h}$, the effective complex envelope vector \vec{g}_m of the MSFVW dynamic magnetization \vec{m} in obliquely magnetized metal clad waveguide can also be given as follows:

$$\vec{g}_m = \begin{pmatrix} \frac{\tilde{h}_y(0)}{-ik_s(m_t + 1)} [m_t(-ik_s\chi_{12} + \chi_{13}\alpha_2)A + (-ik_s\chi_{12} + \chi_{13}\beta_2)B] \\ \frac{\tilde{h}_y(0)}{-ik_s(m_t + 1)} [m_t(-ik_s\chi_{22} + \chi_{23}\alpha_2)A + (-ik_s\chi_{22} + \chi_{23}\beta_2)B] \\ \frac{\tilde{h}_y(0)}{-ik_s(m_t + 1)} [m_t(-ik_s\chi_{32} + \chi_{33}\alpha_2)A + (-ik_s\chi_{32} + \chi_{33}\beta_2)B] \end{pmatrix} \quad (2)$$

here $m_t = \frac{v}{q} e^{(\alpha_2 - \beta_2)t}$; $\begin{cases} \tilde{h}_y(l_1) = \frac{i\pi \cdot j_{ks} \cdot \mu_{s1}}{F^{(1)}(k_s)} \\ \tilde{h}_y(0) = \frac{2s\mu_0 \tilde{h}_y(l_1)}{(s\mu_0 - \mu_{s0})e^{-sk_s l_1} + (s\mu_0 + \mu_{s0})e^{sk_s l_1}} \end{cases}$, $j_{ks} = \frac{J \cdot \sin(\frac{k_s w}{2})}{\pi k_s w}$ is the Fourier transform of the uniform current distribution on the microstrip line, $F^{(1)}(k_s) = \left. \frac{\partial(\mu_{sa} - \mu_{sb})}{\partial k} \right|_{k=k_s}$, in which $\mu_{sa} = -s\mu_0 \frac{-\mu_{s2} + s\mu_0 \tanh(sk l_2)}{s\mu_0 - \mu_{s2} \tanh(sk l_2)}$ and $\mu_{sb} = s\mu_0 \frac{\mu_{s0} + s\mu_0 \tanh(sk l_1)}{s\mu_0 + \mu_{s0} \tanh(sk l_1)}$ are surface magnetic permeabilities above and below interfaces of the microstrip line, respectively; $A = \frac{4\pi^2(1 - e^{-\alpha_2 t})}{\alpha_2 t(\alpha_2^2 t^2 + 4\pi^2)}$, $B = \frac{4\pi^2(1 - e^{-\beta_2 t})}{\beta_2 t(\beta_2^2 t^2 + 4\pi^2)}$.

2.2. The MO Bragg Interaction between GOWs and MSWs

For simplicity, the effect of metal layers on GOWs is ignored, which can be reasonable when metal layers are lift off the YIG film sufficiently (typically more than $1 \mu\text{m}$) [8–10]. For the case, the conventional MO coupled-mode equations (CCME) [7] in the air/YIG/GGG (AYG) structure can be used to analyze approximately the MO diffraction effects in the metal clad waveguide.

In the interaction of MSWs and GOWs, by adjusting the direction of the incident light, the four phase-matching conditions in the CCME can almost be satisfied at the same time. In the case, the corresponding incidence angle and DE are, respectively, called as Bragg angle and Bragg DE. And analytic expressions of GOW amplitudes, which are independent of the direction of the incident light, can be obtained from

the obliquely magnetized CCME [7]:

$$\left\{ \begin{array}{l} C_{TM}^{(u)}(L_{MO}) = h_1 e^{r_1 L_{MO}} + h_2 e^{-r_1 L_{MO}} + h_3 e^{r_2 L_{MO}} + h_4 e^{-r_2 L_{MO}} \\ C_{TM}^{(d)}(L_{MO}) = \frac{r_1^2 - m_1}{m_2} (h_1 e^{r_1 L_{MO}} + h_2 e^{-r_1 L_{MO}}) \\ \quad + \frac{r_2^2 - m_1}{m_2} (h_3 e^{r_2 L_{MO}} + h_4 e^{-r_2 L_{MO}}) \\ C_{TE}^{(u)}(L_{MO}) = -\frac{m_8 r_1}{m_5} (h_1 e^{r_1 L_{MO}} - h_2 e^{-r_1 L_{MO}}) \\ \quad - \frac{m_9 r_2}{m_5} (h_3 e^{r_2 L_{MO}} - h_4 e^{-r_2 L_{MO}}) \\ C_{TE}^{(d)}(L_{MO}) = \frac{m_6 r_1}{m_5} (h_1 e^{r_1 L_{MO}} - h_2 e^{-r_1 L_{MO}}) \\ \quad + \frac{m_7 r_2}{m_5} (h_3 e^{r_2 L_{MO}} - h_4 e^{-r_2 L_{MO}}) \end{array} \right. \quad (3)$$

and then the Bragg DE can be calculated by

$$\eta = \left| \left[C_{TM}^{(d)}(L_{MO}) \right]^2 \right| + \left| \left[C_{TE}^{(d)}(L_{MO}) \right]^2 \right| \quad (4)$$

because the four kinds of the frequency-unshifted and -shifted of the *TM* and *TE* light are coupled each other in the obliquely magnetized waveguide. The parameters shown in Equations (3) and (4) are given as follows: $C_{TM}^{(\cdot)}(x)$ and $C_{TE}^{(\cdot)}(x)$ designate the complex amplitudes of transverse electric field components of the *TM* and *TE* modes, the superscripts (*u*) and (*d*) designate the frequency-unshifted and -shifted light; L_{MO} is the MO interaction length; and

$$\begin{aligned} m_1 &= \kappa_{zy}^{DC} \kappa_{yz}^{DC} + \kappa_{zy}^{AC} \left(\frac{1 \rightarrow}{2} g_m \right) \kappa_{yz}^{AC} \left(\frac{1 \rightarrow^*}{2} g_m \right), \\ m_2 &= \kappa_{zy}^{DC} \kappa_{yz}^{AC} \left(\frac{1 \rightarrow}{2} g_m \right) + \kappa_{yz}^{DC} \kappa_{zy}^{AC} \left(\frac{1 \rightarrow}{2} g_m \right) \\ m_3 &= \kappa_{zy}^{AC} \left(\frac{1 \rightarrow^*}{2} g_m \right) \kappa_{yz}^{DC} + \kappa_{zy}^{DC} \kappa_{yz}^{AC} \left(\frac{1 \rightarrow^*}{2} g_m \right), \\ m_4 &= \kappa_{zy}^{AC} \left(\frac{1 \rightarrow^*}{2} g_m \right) \kappa_{yz}^{AC} \left(\frac{1 \rightarrow}{2} g_m \right) + \kappa_{zy}^{DC} \kappa_{yz}^{DC}, \\ m_5 &= \kappa_{zy}^{AC} \left(\frac{1 \rightarrow^*}{2} g_m \right) \kappa_{yz}^{AC} \left(\frac{1 \rightarrow}{2} g_m \right) - \left(\kappa_{zy}^{DC} \right)^2, \\ m_6 &= \kappa_{zy}^{AC} \left(\frac{1 \rightarrow^*}{2} g_m \right) - \frac{\kappa_{zy}^{DC}}{m_2} (r_1^2 - m_1), \end{aligned}$$

$$\begin{aligned}
m_7 &= \kappa_{zy}^{AC} \left(\frac{1}{2} \vec{g}_m^* \right) - \frac{\kappa_{zy}^{DC}}{m_2} (r_2^2 - m_1), \\
m_8 &= \kappa_{zy}^{DC} - \frac{\kappa_{zy}^{AC} \left(\frac{1}{2} \vec{g}_m \right)}{m_2} (r_1^2 - m_1), \\
m_9 &= \kappa_{zy}^{DC} - \frac{\kappa_{zy}^{AC} \left(\frac{1}{2} \vec{g}_m \right)}{m_2} (r_2^2 - m_1); \\
r_1 &= \sqrt{\frac{(m_1 + m_4) + \sqrt{\Delta_m}}{2}}, \quad r_2 = \sqrt{\frac{(m_1 + m_4) - \sqrt{\Delta_m}}{2}},
\end{aligned}$$

$\Delta_m = (m_1 - m_4)^2 + 4m_2m_3$; $\kappa_{ij}^{AC} \left(\frac{1}{2} \vec{g}_m \right)$, $\kappa_{ij}^{AC} \left(\frac{1}{2} \vec{g}_m^* \right)$ and $\kappa_{ij}^{DC} (i, j = y, z)$ are defined as the Ref. [7], \vec{g}_m can be obtained from the Equation (2); for the TM incident light, $h_1 = h_2 = \frac{m_1 - r_2^2}{2(r_1^2 - r_2^2)}$ and $h_3 = h_4 = \frac{r_1^2 - m_1}{2(r_1^2 - r_2^2)}$; and for the TE incident light, $h_1 = -h_2 = \frac{m_5 m_7}{2r_1(m_6 m_9 - m_7 m_8)}$ and $h_3 = -h_4 = \frac{-m_5 m_6}{2r_2(m_6 m_9 - m_7 m_8)}$.

3. CALCULATION AND DISCUSSION

For the practical MO waveguides used generally in Bragg diffraction experiments, the thickness of the GGG substrate is several hundred times larger than that of the ferrite and the microstrip line transducers are directly deposited on the YIG film for the high excitation efficiency. In this case, the waveguide structure mentioned above is reduced into the metal/dielectric/YIG/GGG (MDYG) four-layered waveguide with $l_1 = 0$ and $l_{-1} \rightarrow \infty$, which will be considered in the following. To compare with the experiment data and theoretical analyses, the parameters are taken from the experiment by Young and Tsai [11]: the wavelength of incident TM₀ light is 1.317 μm; the thickness of YIG is 9 μm, the width and length of microstrip line conductor are 24 μm and 8.8 mm, respectively; the dc applied magnetic field H_0 is 279 kA/m, the anisotropic field is 16 kA/m, and the saturation magnetization M_0 is 139 kA/m; the refractive indices of YIG and GGG are 2.2 and 1.59, respectively; the MO coefficients are $f_1 = 2.44 \times 10^{-9} \text{ (A/m)}^1$, $f_{44} = 5.84 \times 10^{-15} \text{ (A/m)}^2$, $\Delta f = -2.92 \times 10^{-15} \text{ (A/m)}^2$.

In what follows, the MO interaction in metal clad YIG waveguides is discussed; and then the dependences of the Bragg DE and the -3 dB bandwidth on the spacing of the metal layer from the YIG film are presented; finally, the gain-bandwidth product is analyzed in the different spacing and inclination angle.

3.1. Metal Layer Effects on the MO Bragg Interaction

The Bragg DE η calculated by the Equation (4) is shown in Fig. 2(a), in which the relative dielectric thickness R is defined by $R = l_2/t$. The experiment data [11] consist with our theoretical results at $R = \infty$ in the normal magnetization ($\theta = \varphi = 0^\circ$). It is clear from Fig. 2(a) that: (1) the presence of the metal layer decreases the DEs at lower frequency end and then the MO -3 dB bandwidth $B_{-3\text{dB}}$; (2) by properly adjusting the relative dielectric thickness R , the Bragg DEs can be improved comparison with the case of the conventional AYG waveguide; (3) and the frequency f_P corresponding to the peak Bragg DE η_p can be tunable by the spacing of the metal layer from the YIG film. The dependence of the frequency f_P on the relative dielectric thickness R is shown in Fig. 2(b). The range of the frequency f_P almost covers the whole MO -3 dB bandwidth of the case without metal layers, which means that the DE improvement can be obtained in the frequency range of interest.

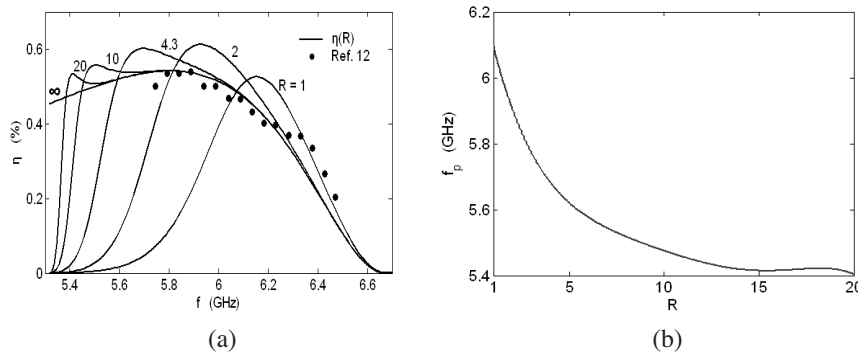


Figure 2. (a) The Bragg DEs in different waveguide configurations, (b) the dependence of the frequency f_P on the relative dielectric thickness R .

It should be pointed out that the MSFVW group velocities at the frequencies around the f_P are lower than that of the case without metal layers, which can help to obtain the better frequency resolutions and Bragg DEs at the same frequency range in the MO spectrum analyzer. It is also clear that the DE improvement at the normal magnetization is very low, but the metal layer effects on the improvement DE can be increased under the inclined bias magnetic field. The details will be given in the following section.

3.2. The DE Improvement by Metal Layer Effects

The MSFVW frequency range is the function of the inclination angle θ [12]. To compare with the results above, the MSFVW frequency range at 5.46 ~ 7.52 GHz will be discussed corresponding to the inclination angle θ at $0^\circ \sim 21.7^\circ$. In our calculation, the direction of the bias magnetic field is changed while the magnitude keeps fixed. And the inclination angle φ is equal to 180° , because the maximal DE can be achieved in the x - z plane for the case of the noncollinear interaction of GOWs and MSFVWs [12].

For a given inclination angle θ , the relative dielectric thickness R is changed for the DE improvement at one MSFVW frequency. The maximum DE improvement is obtained at $f = 7.52$ GHz, and the dependence of the maximum DE on the inclination angle θ is given in Fig. 3(a). A 7.32 dB improvement is achieved at $\theta = 15.5^\circ$ and $R = 1$. However, the MO -3 dB bandwidth will be decreased as the magnetization direction deviates from the z axis and the metal layer are close to the YIG film, and the results are shown in Fig. 3(b). When the maximum DE improvement is obtained, the MO bandwidth is dropped down to 140 MHz. Thereby a more comprehensive evaluation should be given for a MO Bragg cell.

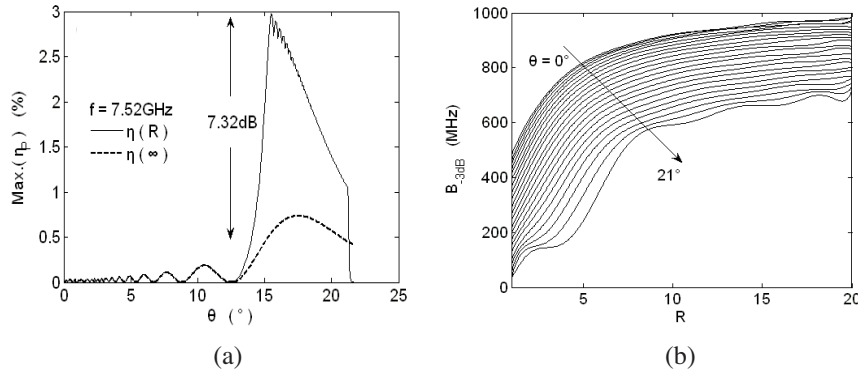


Figure 3. (a) The dependence of the maximum DE on the inclination angle θ , (b) the MO -3 dB bandwidth $B_{-3\text{dB}}$ in different obliquely magnetized waveguides.

The gain-bandwidth product defined by $G_\eta \times B_{-3\text{dB}} = 10 \times \lg\left(\frac{\eta_p(R)}{\text{Max}(\eta(\infty))}\right) \times B_{-3\text{dB}}$ (dB·MHz) at a given magnetization direction is a proper parameter to evaluate metal layer effects on Bragg DEs and MO bandwidths synthetically. The dependence of the gain-bandwidth product on the relative dielectric thickness R and the inclination angle

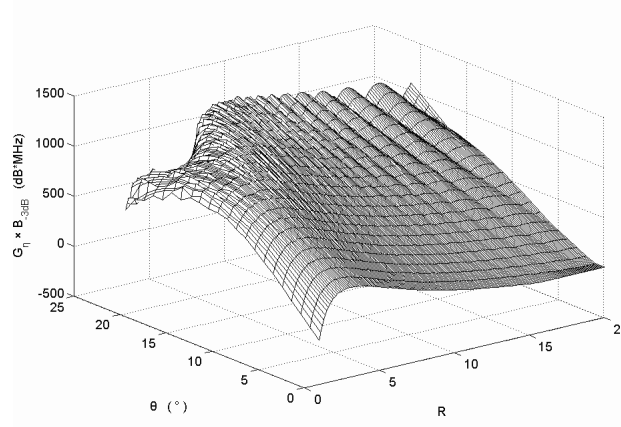


Figure 4. The dependence of the gain-bandwidth product on the relative dielectric thickness R and the inclination angle θ .

θ is shown in Fig. 4. When the gain-bandwidth product is up to the maximum, the DE improvement $G_{\eta}(R = 8.4)|_{\theta=21^{\circ}}$ is equal to 3.9 dB and the -3 dB bandwidth is 560 MHz. Almost 70% MO bandwidth is kept comparing with the case without metal layers, and the maximum DE improvement of 3.9 dB is also obtained.

4. CONCLUSION

The MSFVW dispersion relation and the dynamic magnetization in the obliquely magnetized metal clad YIG waveguide are obtained by the method of the surface magnetic permeability, and the noncollinear Stokes interaction between the GOWs and the MSFVWs is discussed according to analytic expressions of the MO coupled-mode equations. By analyzing the diffraction process of the GOWs with the MSFVWs in the MDYG waveguide, it is known that: (1) the MO diffraction efficiency can be improved by a proper selection of the spacing between the YIG film and metal layer, and the maximum DE improvement of 7.32 dB can be obtained; (2) the gain-bandwidth product can be used to evaluate the metal effects on the Bragg DE and the MO bandwidth synthetically, and the 3.9 dB improvement and 560 MHz bandwidth are achieved when the product is up to the maximum.

ACKNOWLEDGMENT

This work was supported by National Nature Science Foundation of China (60671027).

REFERENCES

1. Daniel, M. R., J. D. Adam, and T. W. O'Keefe, "Linearly dispersive delay lines at microwave frequencies using magnetostatic waves," *IEEE Ultrasonics Symposium Proc.*, 806–809, 1979.
2. Adam, J. D., T. W. O'Keefe, and M. R. Daniel, "Magnetostatic wave devices for microwave signal processing," *SPIE Real-Time Signal Proc.*, Vol. 241, 96–103, 1980.
3. Sethares, J. C., J. M. Owens, and C. V. Smith., "M.S.W. nondispersive electronically tunable time delay elements," *Electron. Lett.*, Vol. 16, 825–826, 1980.
4. Ganguly, A. K. and D. C. Webb, "Microstrip excitation of magnetostatic surface waves: theory and experiment," *IEEE Trans. Microwave Theory Tech.*, Vol. 23, 998–1006, 1975.
5. Emtage, P. R., "Interaction of magnetostatic waves with a current," *J. Appl. Phys.*, Vol. 49, 4475–4484, 1978.
6. Wu, B.-J., "Analysis of mode characteristics of microwave magnetostatic waves," *Journal of Microwares*, Vol. 22, 5–7, 2006.
7. Wu, B.-J. and K. Qiu, "An effective method for improving diffraction performance of magnetostatic backward volume wave based magneto-optic Bragg cells by using an appropriately titled bias magnetic field in YIG film plane," *J. Magn. Magn. Mater.*, Vol. 303, 227–231, 2006.
8. Ma, C. and J. Cao, "TM mode optical characteristics of five-layer MOS optical waveguides," *Opt. Quant. Electron.*, Vol. 26, 877–884, 1994.
9. She, S. X., "Accurate perturbation analysis of metal-clad and absorptive multilayer dielectric waveguides in near cutoff," *Opt. Commun.*, Vol. 135, 241–246, 1997.
10. Kumar, D., V. K. Sharma, and K. N. Tripathi, "Frequency response of metal clad planar optical waveguides," *Optics Laser Technol.*, Vol. 39, 68–71, 2007.
11. Young, D. and C. S. Tsai, "GHz bandwidth magneto-optic interaction in yttrium iron garnet-gadolinium gallium garnet waveguide using magnetostatic forward volume waves," *Appl. Phys. Lett.*, Vol. 53, 1696–1698, 1988.
12. Wu, B.-J. and K. Qiu, "Magneto-optic coupling theory for guided optical waves and magnetostatic waves using an arbitrarily titled bias magnetic field," *Chin. Phys. Lett.*, Vol. 22, 2396–2399, 2005.